

Short communication

Coexistence of the single chain magnet and spin-glass behavior in a cyano-bridged $\{\text{Fe}^{\text{III}}_2\text{Fe}^{\text{II}}\}$ chain



Liang Zhao, Yan-Juan Zhang*, Ji-Xiang Hu, Cheng-Qi Jiao, Jun-Li Wang, Chun-Ying Duan, Tao Liu*

State Key Laboratory of Fine Chemicals, Dalian University of Technology, Dalian, 116024, China

ARTICLE INFO

Article history:

Received 16 January 2016

Received in revised form 10 February 2016

Accepted 12 February 2016

Available online 15 February 2016

Keywords:

Cyano-bridged

Single chain magnet

Spin-glass

ABSTRACT

A cyano-bridged ferromagnetic $\{\text{Fe}^{\text{III}}_2\text{Fe}^{\text{II}}\}$ alternating chain $\{[\text{Fe}^{\text{III}}(\text{pzTp})(\text{CN})_3]_2[\text{Fe}^{\text{II}}(\text{imidazole})(\text{H}_2\text{O})]\} \cdot 3\text{H}_2\text{O}$ (**1**) (pzTp = tetrakis(pyrazolyl)borate) was synthesized via rational design. Crystal structure analysis studies demonstrated that complex **1** had a one-dimensional double zigzagging chain-like structure. Magnetic measurements showed that ferromagnetic interactions dominate in **1** and the AC magnetic susceptibility revealed two limit regimes in accordance with the single chain magnet and spin-glass behavior.

© 2016 Elsevier B.V. All rights reserved.

Molecular nanomagnets, known as single molecule magnets (SMMs) and single chain magnets (SCMs), that exhibit slow relaxation of their magnetization are attracting considerable interest [1–3]. Such materials not only permitted the observation of fascinating quantum phenomena such as quantum tunneling and finite size effects, but also provided promising applications in high-density information storage, quantum computing, and spintronics [4–6]. The SCMs are especially promising because of their intrinsic structural anisotropy and virtual infinite spin ground state. Since Glauber predicted the existence of the SCM in 1963 and D. Gatteschi first synthesized the one-dimensional (1D) systems displaying slow magnetic dynamics in an experimental method in 2001, many new experimental systems have been developed [7–9]. Actually, it is still a challenge to construct such complexes because the low dimension structure, strong uniaxial magnetic anisotropy, strong intrachain interaction and weak interchain interactions are necessary [10,11]. It is a complicated task to mix those elements together into one complex. Up to date, several useful strategies have been reported to construct SCMs, such as choosing the big steric hindrance ligand modificatory metalocyanate building block to reduce the dimension of the complex and enhance the intrachain interaction; selecting transition metal ions (Fe^{2+} , Co^{2+} , Ni^{2+} , Mn^{3+}) to meet the need of strong uniaxial magnetic anisotropy and choosing reasonable organic ligand in order to adjust the ligand field of the ions and weaken the interaction between the different chains [12–15]. According to this strategy, we choose $[\text{Fe}(\text{pzTp})(\text{CN})_3]^-$ (pzTp = tetrakis(pyrazolyl)borate) as a building block, which has moderate steric effects, to provide suitable interchain magnetic interactions and strong intrachain interactions [14,16]. Moreover, it has been reported that interactions between low-spin

Fe^{III} and high-spin Fe^{II} are generally ferromagnetic, preferring a high-spin state that benefits SCM behavior [13]. Therefore, we successfully synthesized a complex $\{[\text{Fe}^{\text{III}}(\text{pzTp})(\text{CN})_3]_2[\text{Fe}^{\text{II}}(\text{imidazole})(\text{H}_2\text{O})]\} \cdot 3\text{H}_2\text{O}$ (**1**) by the self-assembly reaction of $[\text{Fe}(\text{pzTp})(\text{CN})_3]^-$ building block, Fe^{2+} ion and imidazole that presented two relaxation regimes attributed to SCM and spin-glass behaviors.

The target complex **1** was synthesized by a diffusion method in a test tube [17]. Single crystal X-ray diffraction analysis revealed that complex **1** crystallizes in a triclinic $P\bar{1}$ space group. As shown in Fig. 1, the crystal structure comprises neutral bimetallic double-zigzag $[\text{Fe}^{\text{III}}(\text{pzTp})(\text{CN})_3]_2[\text{Fe}^{\text{II}}(\text{imidazole})(\text{H}_2\text{O})]$ chains with three uncoordinated water molecules located between them [18,25]. In the neutral chain, the $[\text{Fe}^{\text{III}}(\text{pzTp})(\text{CN})_3]^-$ unit bridged one $[\text{Fe}^{\text{II}}(\text{imidazole})_2]^{2+}$ and one $[\text{Fe}^{\text{II}}(\text{H}_2\text{O})_2]^{2+}$ unit through two of its three cyanide groups in the *cis* position, whereas each $[\text{Fe}^{\text{II}}(\text{imidazole})_2]^{2+}$ or $[\text{Fe}^{\text{II}}(\text{H}_2\text{O})_2]^{2+}$ unit linked two $[\text{Fe}^{\text{III}}(\text{pzTp})(\text{CN})_3]^-$ units, forming a bimetallic double-zigzag chain that run parallel to the *b* axis. Four metal ions of the $\{\text{Fe}^{\text{III}}_2\text{Fe}^{\text{II}}_2\}$ units present a folded square with the dihedral angles of 32.23° formed between the planes of the triangular $\text{Fe}^{\text{III}}_2\text{Fe}^{\text{II}}$ units owing to the steric effect of the bulky $[\text{Fe}(\text{pzTp})(\text{CN})_3]^-$ building blocks. The crystal structure contains four unique iron centers. Each Fe^{I} and Fe^{III} center is coordinated to two nitrogen atoms from the pzTp units and three cyanide carbon atoms and each Fe^{II} center is coordinated to two nitrogen atoms from the imidazole ligand in the axis position and four cyanide carbon atoms in the equatorial position. The apical and equatorial positions of the Fe^{II} center were occupied by two water oxygen atoms and four cyanide carbon atoms. The coordination geometries of all the iron sites are octahedron (D_{4h}). At 300 K, the $\text{Fe}^{\text{II}}-\text{N}_{\text{equatorial}}$ bond lengths were 2.122–2.133 and 2.090–2.102 Å for Fe^{II} and Fe^{I} , and the $\text{Fe}^{\text{II}}-\text{N}_{\text{apical}}$ and $\text{Fe}^{\text{I}}-\text{O}_{\text{apical}}$ distances were 2.171 and 2.126 Å, respectively. The $\text{Fe}^{\text{III}}-\text{C}$ distances were 1.889–1.908 and

* Corresponding authors.

E-mail addresses: yanjuan Zhang@dlut.edu.cn (Y.-J. Zhang), liutao@dlut.edu.cn (T. Liu).

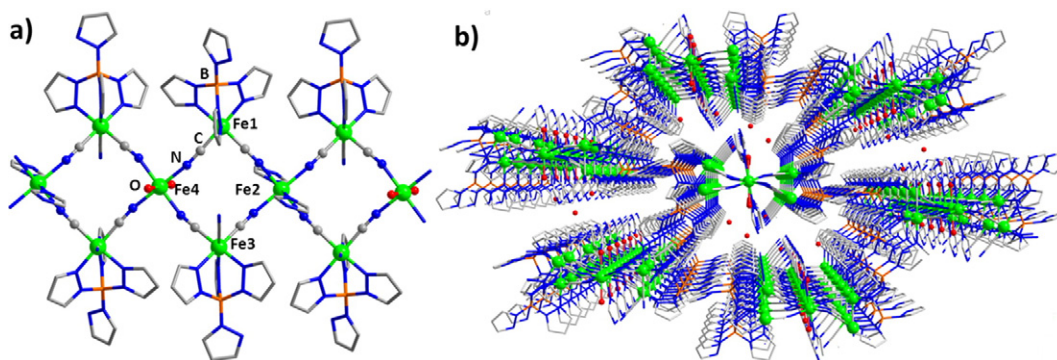


Fig. 1. (a) Perspective view of one-dimensional zigzag infinite chains of **1**; (b) Packing diagram of **1** along the *b*-axis. H atoms have been omitted for clarity (Fe, light green, C, gray, N, blue, B, orange, O red).

1.891–1.901 Å and the Fe^{III}–N distances were 1.958–1.973 for Fe1 and 1.959–1.978 Å for Fe3, respectively. The structural parameters indicate that the Fe^{II} and Fe^{III} centers correspond to high and low spin states [19,20]. The shortest interchain metal–metal distance is 11.115 Å, providing the possibility to diminish the interchain magnetic interactions and satisfy the requirements for SCM. The intermolecular hydrogen-bonding interactions were formed between oxygen atoms of coordinated water molecules and lattice water molecules, which played an important role in improving the stability of the network and affecting the magnetic property.

Magnetic measurements were conducted using a superconducting quantum interference device (SQUID) magnetometer (Quantum Design MPMS-7). Variable-temperature magnetic measurements were performed on polycrystalline samples of complex **1** in the range of 1.8–300 K under a dc field of 1000 Oe. As shown in Fig. 2(a), the χT value per {Fe^{III}₂Fe^{II}} unit was 5.23 cm³ mol⁻¹ K at 300 K. This value was higher than the spin-only value expected for two isolated Fe^{III} of $S = 1/2$ ($g = 2.0$) and two Fe^{II} of $S = 2$ ($g = 2.0$) due to the orbital contributions of Fe^{II} ions. As cooling, the χT values remain nearly constant between 300 and 40 K and then gradually increased to a sharp maximum of 105.31 cm³ mol⁻¹ K around 5.2 K, indicating the ferromagnetic interactions between Fe^{III} and Fe^{II}. The Curie–Weiss fit of the magnetic susceptibility data in the temperature range of 10–300 K, gave Curie constant and Weiss constant of 4.99 cm³ mol⁻¹ K and 9.89 K, respectively. The positive Weiss constant confirms that the ferromagnetic coupling interactions are dominant in the chain complex. As the temperature further lowered, the χT value dropped sharply to 46.8 cm³ mol⁻¹ K at 1.8 K. The sudden decrease in χT is attributed to the presence of zero-field splitting and/or antiferromagnetic interactions.

At 1.8 K, the isothermal magnetization increased rapidly below 1 kOe and then linearly to 5.9 $N\beta$ at 50 kOe on increasing the applied magnetic field (Fig. 2(b)), which agrees with the predicted saturation value of 6.0 $N\beta$. The zero-field-cooled (ZFC) and field-cooled (FC) magnetization measurements were performed for **1** at 10 Oe in the 2–10 K range to research the phase transformation at low temperatures. The curves show a divergence at 3.8 K, indicating slow relaxation of magnetization at temperatures below 3.8 K (Fig. S2).

To investigate the possibility of SCM behavior, we studied ac magnetic susceptibility as a function of both temperature and frequency (Fig. 3(a)). The in-phase (χ') and out-of-phase (χ'') showed apparent frequency dependency in two temperature regions ranging of 1.8–3.2 and 2.3–4.9 K, with the peak maxima shifting to higher temperatures as the frequency increased. For the relaxation process in low temperature (LT), the parameter $\phi = (\Delta T_p/T_p)/\Delta(\log f)$, a measure of the frequency dependence of the peak temperature shift (ΔT_p) of χ'' , was estimated to be 0.15, is out of the range for spin-glass but lies in the expected range for a superparamagnet ($\phi > 0.1$), and thus rules out the possibility of spin-glass behavior. Moreover, the relaxation rate can be simulated by the Arrhenius equation $\tau = \tau_0 \exp(\Delta/k_B T)$, where $\tau = 1/2\pi\nu$ and τ_0 was a pre-exponential factor. Least-squares fitting gives $\tau_0 = 2.50 \times 10^{-9}$ s and $\Delta/k_B = 28.3$ K (Fig. 3(b)). The above results suggest that the interchain magnetic interactions did not suppress the spin relaxation of the chain. These values are in good agreement with those reported values for typical SCMs [21]. For an anisotropic chain, the χT followed the equation $\chi T/C_{eff} = \exp(\Delta_\zeta/k_B T)$, where C_{eff} is the effective Curie constant and Δ_ζ is the energy required to create a domain wall along the chain. The $\ln(\chi T)$ vs. $1/T$ plot for **1** between 6.2 and 300 K shows a linear region with a slope of $\Delta_\zeta/k_B = 18.37$ K (Fig. 3(c)). At 5.1 K, $\ln(\chi T)$ reaches a

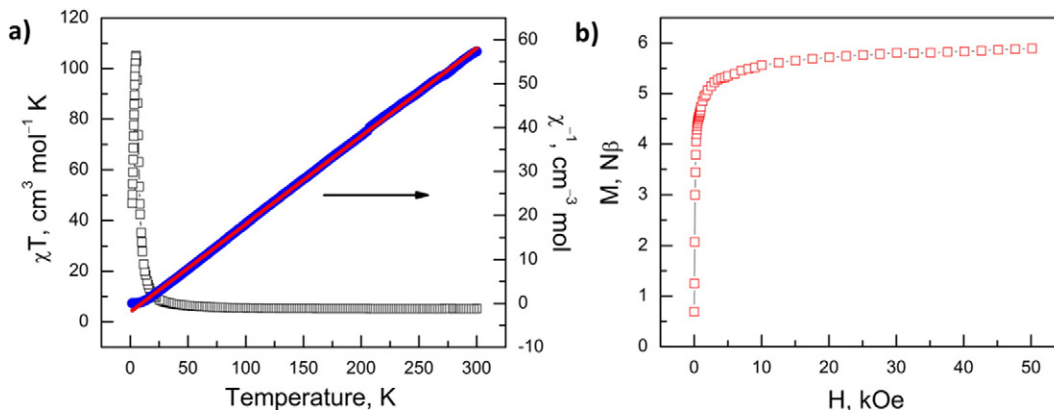


Fig. 2. (a) Temperature-dependent magnetic susceptibility for **1**; Red lines represent the best fit of the Curie–Weiss results. (b) Field dependence of magnetization of **1** at 1.8 K.

Download English Version:

<https://daneshyari.com/en/article/1305286>

Download Persian Version:

<https://daneshyari.com/article/1305286>

[Daneshyari.com](https://daneshyari.com)